Vol. 20, n.° 4, pp. 45-58, 2021
Revista UIS Ingenierías
Journal homepage: https://revistas.uis.edu.co/index.php/revistauisingenierias

Algorithm for the joint analysis of the ECG and PPG signals

Algoritmo para el análisis en conjunto de las señales del ECG y PPG

Diana Carolina Martínez-Reyes [1]

[1] Grupo de Investigación en Aplicaciones Mecatrónicas (GRAM), Facultad de Ingeniería Mecatrónica, Universidad Santo Tomás, Colombia. Email: diana.martinez@ustabuca.edu.co. Orcid: 0000-0001-7899-1770.

Received: 10 November 2020. Accepted: 16 February 2021. Final version: 21 June 2021.

Abstract

The main objective of this research is based on finding out some assertive and robust Photoplethysmogram's PPG & Electrocardiogram's ECG blood pressure-related parameters by the implementation of a novel method with innovations in signal processing and analysis. The biomedical ECG and PPG signals are recorded using a mobile monitor CardioQVark. To increase the cuffless blood pressure measurement accuracy, a technique that involves not only the ECG and PPG joint parameters extraction but also some individual PPG's morphology features, is proposed in this work. Firstly, the biomedical ECG and PPG signals are time–frequency filtered. Secondly, some novel parameters from the morphology of photoplethysmogram signal, which may be correlated with blood pressure, are considered in addition to the pulse transit time. Additionally, a neural network is built to determine the relationship between the estimated and reference blood pressure. Finally, the correlation coefficient and regression line are obtained to evaluate the feasibility.

Keywords: blood pressure; Electrocardiogram; mobile monitor; Photoplethysmogram; PPG morphology; PTT.

Resumen

El objetivo de esta investigación consiste en identificar aquellos parámetros provenientes de las señales del electrocardiograma ECG y fotopletismograma PPG que permitan hacer una evaluación de la presión sanguínea utilizando un dispositivo móvil. El método propuesto incluye innovaciones en el procesamiento y análisis de las señales. Con el objetivo de aumentar la precisión de la medición de la presión sanguínea, en este trabajo, se propone la utilización de parámetros provenientes de la señal del PPG en conjunto con el PTT obtenido de las señales del ECG y PPG analizadas en conjunto. Adicionalmente, se propone el diseño e implementación de una red neural para determinar la relación existente entre la presión sanguínea estimada por el método y la de referencia, lo cual permite evaluar la viabilidad del método propuesto.

Palabras clave: presión sanguínea; electrocardiograma; monitor móvil; fotopletismografia; PTT.

1. Introduction

Hypertension is a major risk indicator for coronary heart diseases, which according to the world health organization corresponds to the primary global risk of mortality [1]. Blood pressure (BP) measurement, including systolic blood pressure (SBP) and diastolic blood pressure (DBP), is an important vital sign of health care and represents a fundamental biomedical signal for managing the risks associated with hypertension.

Today, the most common practice for blood pressure measurement is the oscillometric technique due to its primitiveness and availability.

ISSN Printed: 1657 - 4583, ISSN Online: 2145 - 8456,
How to cite: D. Carolina Martínez-Reyes, "Algorithm for the joint analysis of ECG and PPG signals," *Rev. UIS Ing.*, vol. 20, no. 4, pp. 45-58, 2021, doi: 10.18273/revuin.v20n4-2021004.

One of the problems demonstrated with this practice is the so-called 'white coat effect', that represents an increase in the blood pressure of the patient in the presence of a physician. While the oscillometric technique can be used at home and in this case, it promises to show a more accurate measurement where it requires the use of a cuff that limits the self-recording of BP.

In addition, literature has shown that most cardiovascular parameters (heart rate, blood pressure, artery resistance) are linked and may be correlated with the feature in photoplethysmogram signal, which reveals the changes of blood volume during a cardiac cycle [2].

Considering these observations, researchers have been developing techniques based on electrocardiogram (ECG) and photoplethysmogram (PPG) signals for blood pressure measurement in which various methods are used to extract different features as the PTT and other morphological features as the ones presented in [3].

Although the current methods exhibit high fidelity in terms of BP estimation, they require high sensor synchronization as they are based on pulse wave velocity (PWV). Furthermore, they lack applicability in different scenarios.

Consequently, in this paper, we propose a method based on continuous wavelet transform for signal processing. Moreover, to assess BP we consider some parameters from the morphology of the PPG signal besides the PTT. At the last stage, a feed-forward neural network is designed and implemented to construct the regression line and correlation coefficient between the reference and estimated BP, thus evaluating feasibility.

2. Materials and methods

2.1. Devices and experimental procedure

The data collection involves the recording of the ECG and PPG signals from the mobile cardio monitor CardioQvark [4] for three minutes (Figure 1).

This device obtains the biomedical signals at a sample rate of 1000 Hz. Additionally, the SBP and DBP are measured from a conventional sphygmomanometer (Figure 2), and its information is retrieved with the ECG and PPG signals.

An average of twenty recordings is measured from each of the eleven patients. The patient's age range is within thirty to seventy years (30 to 70) and the overall health condition varies among them.

Figure 1. Patient holding the cardioQVark. Source: [3].

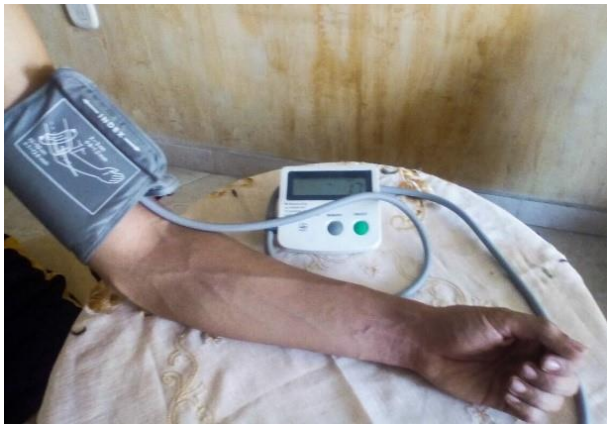

Figure 2. Reference BP measurement. Source: authors.

2.2. Signal processing

Previous signal processing methods required a process to get rid of the unwanted information coming from motion artifacts and power lines, which might compromise the quality of the signals.

Firstly, once the data is collected, it is organized in tables where the patient's ID, blood pressure measurements, ECG, and PPG recordings are gathered and imported into the Matlab workspace (Figure 3).

Secondly, from the raw ECG signal, an algorithm is used to identify the QRS complexes and further establish the patient's heart rate (HR).

To accomplish this, the first algebraic derivative of the raw ECG signal is obtained to accentuate the R wave slope [5].

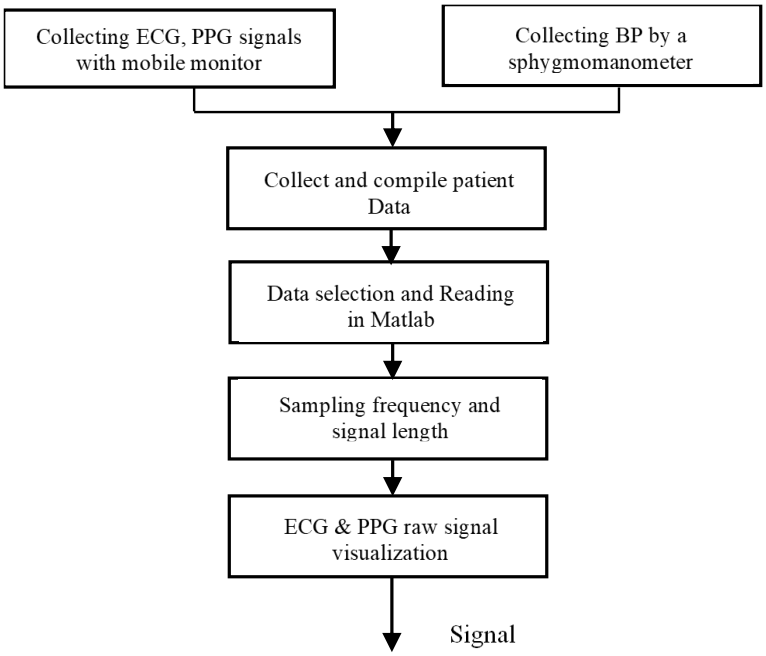

Figure 3. Signal preprocessing. Source: authors.

Secondly, an amplitude threshold is set based on the first derivative maximum and mean values. Then, the peaks exceeding the limits are considered as R peaks. Using a threshold enables the adjustment of signal changing conditions automatically since thresholds float over the noise.

The common cardiac cycle rate range is from 60 to 120 beats per minute [6], thus, once the first R peak is identified, it is expected that a minimum amount of time should elapse before the subsequent R peak arises. Therefore, a sliding window in the time domain is implemented besides the amplitude threshold.

Consequently, the peak candidate that exceeds the magnitude threshold and the time dead zone are denoted as R peaks. The following workflow shows the algorithm for the QRS identification process (Figure 4).

Figure 5 shows an example of the R peak detection. In the upper box, the ECG first derivate, below the dead zone interval with the R peak detected.

Although regarding algorithm's accuracy, in some cases, the R peak is not exactly identified, the imprecision does not exceed a ten samples difference. This work does not aim to deeply study the QRS complex but just to use the R peak to obtain an R-R interval which will give enough information to segment the signal in cycles.

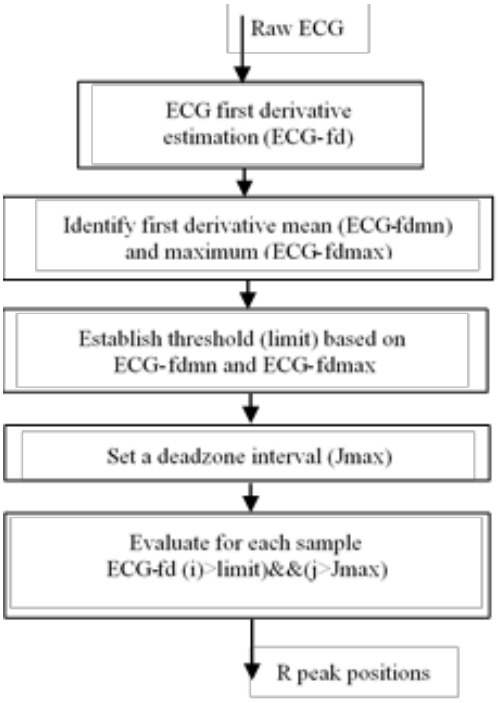

Figure 4. QRS complex identification process. Source: authors.

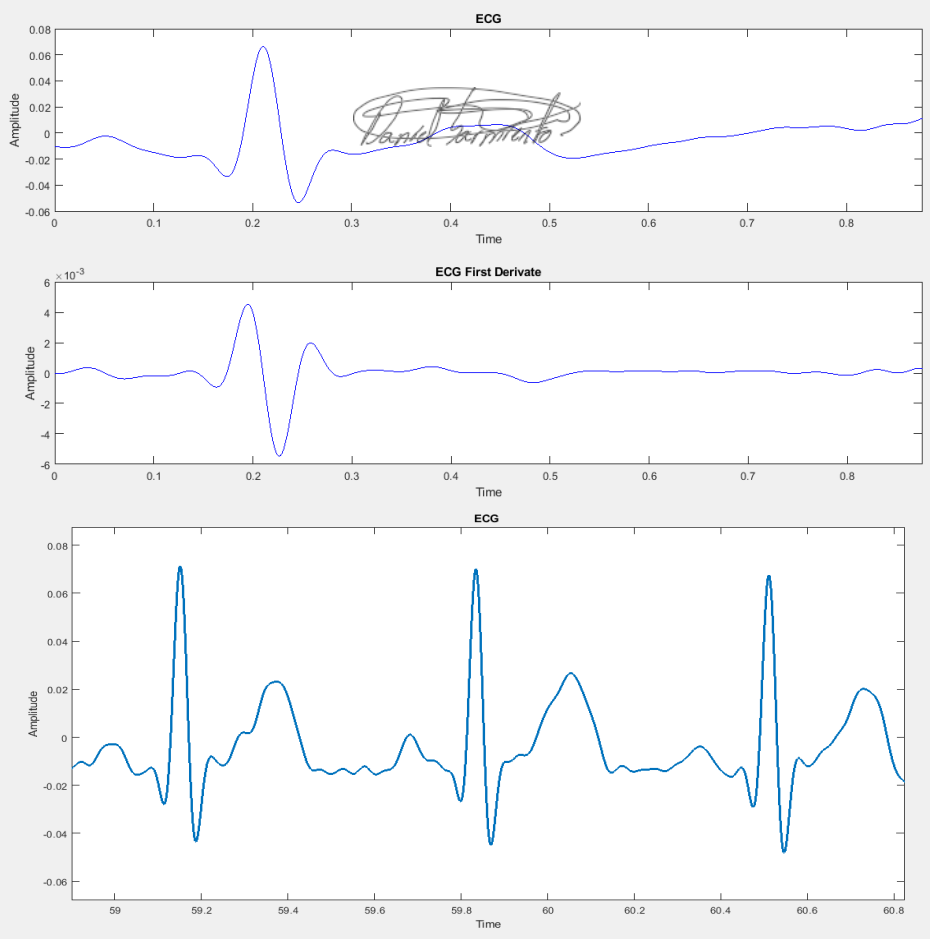

Figure 5. QRS complex identification example. Source: authors.

2.3. Signal processing ECG & PPG Time-Frequency analysis

Wavelet analysis is arising as a powerful tool for the processing of non-stationary signals [7]. They describe the temporal characteristics of a signal by its spectral components in the frequency domain.

The wavelet transform (WT) is a signal decomposition onto a set of basic functions. For the design of the WT procedure, there are two important functions, which need to be described: the scaling function and the primary wavelet function.

The scaling function dilates or narrows the signal and is related to the levels of decomposition of the signal. For instance, in the first decomposition level, a scale of two is applied and the signal sampling frequency is divided in two. Then in the second decomposition level, the signal sampling frequency is scaled by a factor of four [8].

Figure 6 shows the time-frequency representation of the ECG signal after applying the wavelet transform. It can be observed that the fluctuating features, which contain the important ECG information, lie in the frequency range between 8 to 32 Hz. Therefore, the components exhibited at lower frequencies are considered as the artifacts related to patient's movement and the ones exposed at higher frequencies are noise from power lines.

The WT is also applied to the raw PPG signal and the results are presented in Figure 7. Applying the same interpretation as the one for ECG signal, the main PPG information is found between the frequency range 2 to 10 Hz. Lower and higher-frequencies features are taken as noise.

In this work, we contemplate that as the patient's heart rate (HR) changes, so does the ECG beat-to-beat interval. For that reason, we use an adaptive frequency range to extract the signal information, in which the boundaries are set in terms of the HR retrieved from the R–R interval that we got in the preprocessing step [9].

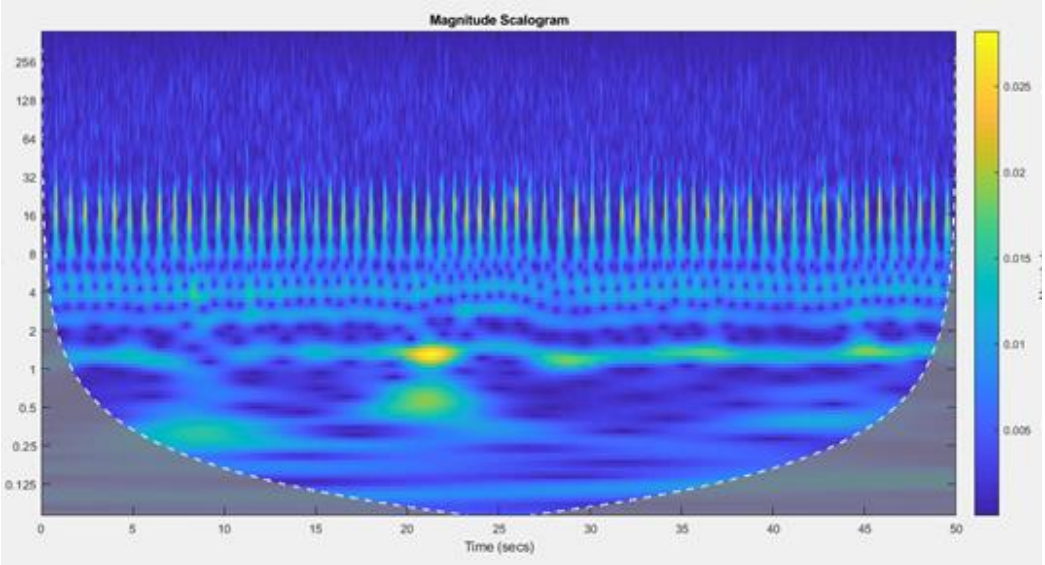

Figure 6. ECG scalogram. Source: authors.

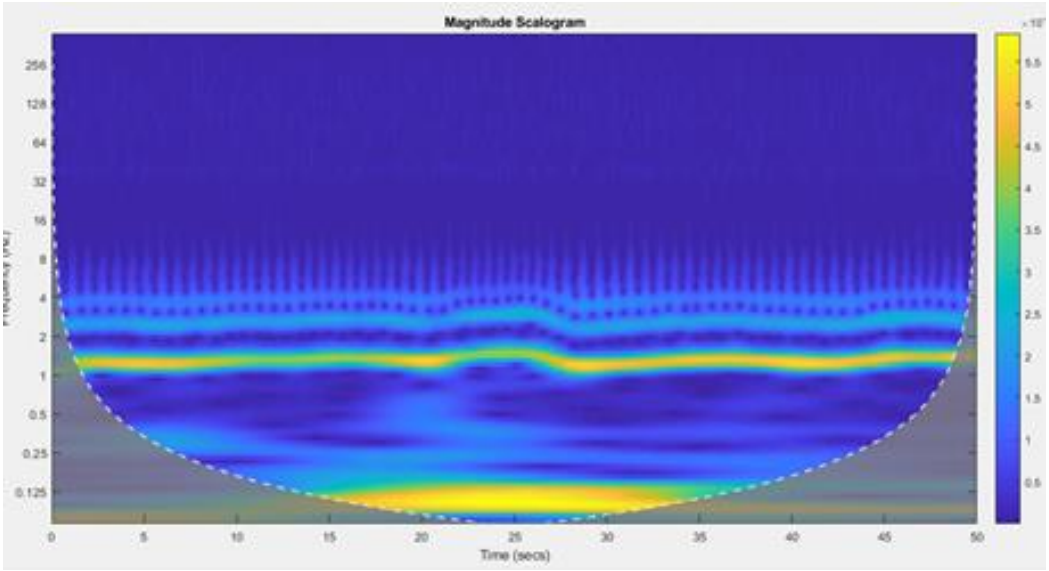

Figure 7. PPG scalogram. Source: authors.

After the time–frequency representation of the biomedical ECG and PPG signals and the identification of the spectral range where the meaningful information stays, the reconstruction process starts. In this step, the inverse continuous wavelet transform (ICWT) is used to assemble selected signal components back into the original with no loss of information. In Figure 8, the reconstructed and raw ECG signals are presented. For the assembly of the signal, the baseline drift is corrected by removing the frequency components, which coincide with motion artifacts or low-frequency noises. Additionally, artifacts coming from power lines, or high-frequency noises were identified and discarded to get a filtered and baseline corrected signal.

In the case of the PPG signal, after the time–frequency representation and analysis, the reconstruction signal is done using the ICWT and the reconstruction frequency range is established in such a way that the identified baseline wander components and captured high frequencies noises are extracted (Figure 9).

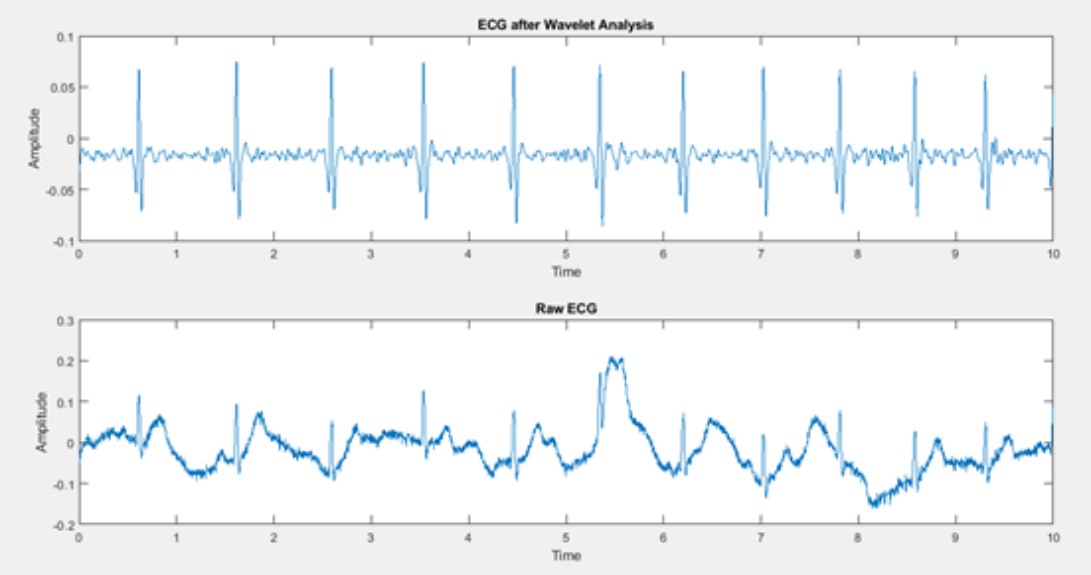

Figure 8. ECG signal after WT and Raw ECG. Source: authors.

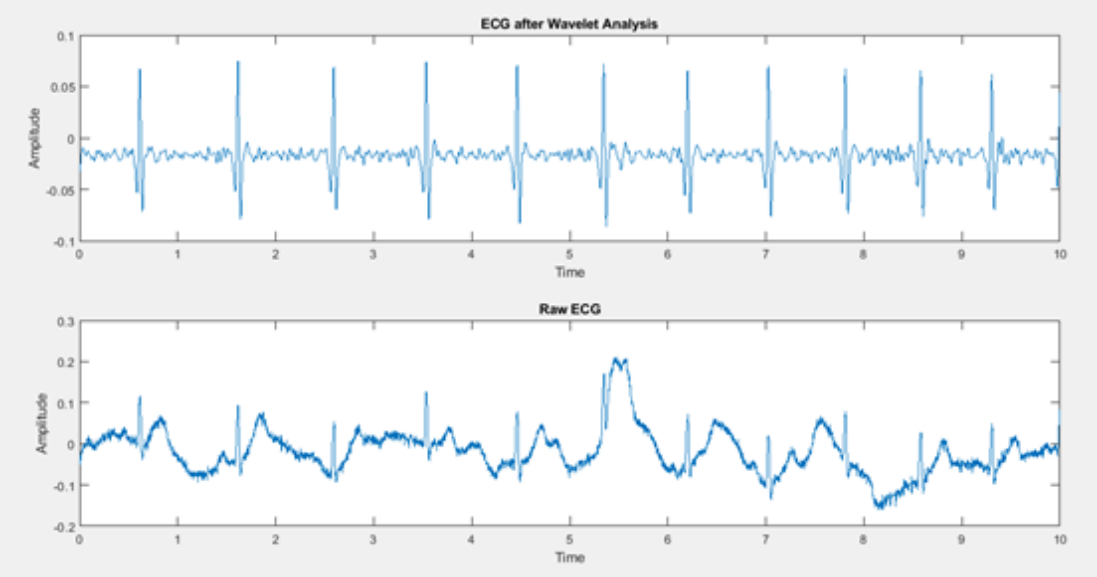

Figure 9. PPG signal after WT and Raw PPG. Source: authors.

2.4. Signal analysis

After processing the biomedical signals, the corresponding single cycle waveform model needs to be selected for the intent of feature extraction.

To obtain the PPG's waveform single cycle which best describes the whole signal, the R-R interval is used to reshape the signal in terms of one period. In other words, the signal, which initially was described in a vector, is organized in a matrix in which one row represents the data for one signal period.

The number of rows depends on the length of the signal and the R – R interval magnitude.

Secondly, a matrix with the correlation coefficients between the cycles is obtained to be able to evaluate which cycles are strongly correlated.

Finally, the group of signals that are highly associated is gathered in the signal group models (Figure 10). As a result of the process, the single-cycle PPG waveform presented in Figure 11 is obtained.

In contemplation of the synchronization requirement between the PPG and ECG biomedical signals are presented. After identifying the cycles which best describe the PPG signal or group models, the same time localized cycles corresponding to the ECG signal are extracted, and the corresponding model is obtained (Figure 12).

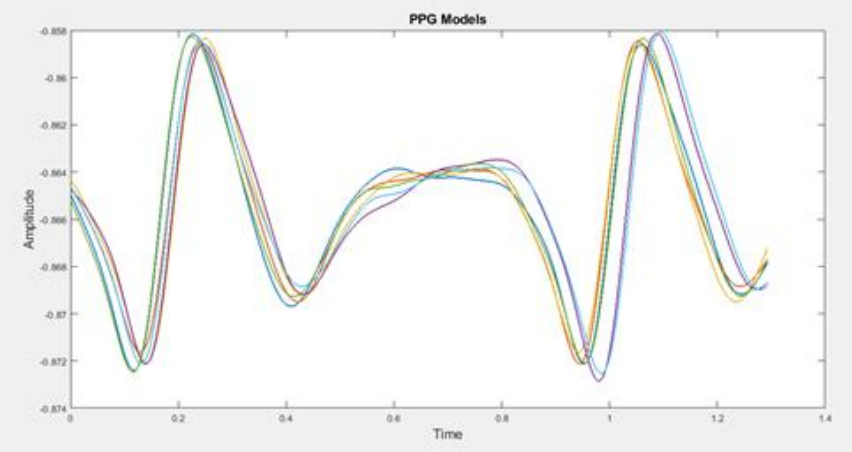

Figure 10. PPG signal group models. Source: authors.

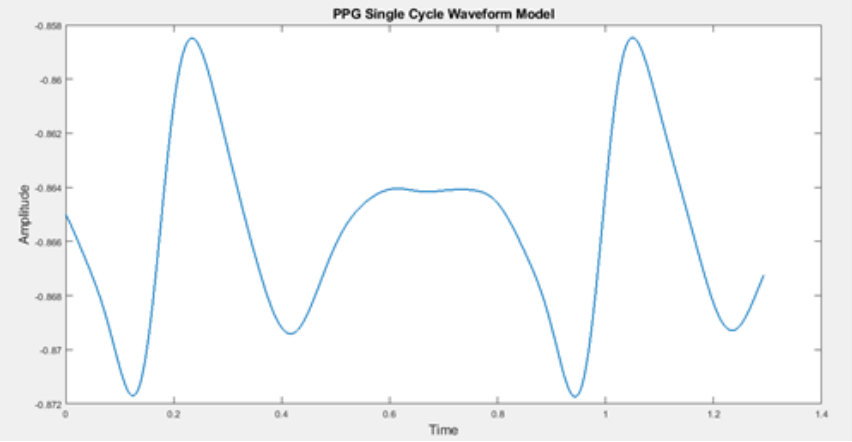

Figure 11. PPG Single cycle model. Source: authors.

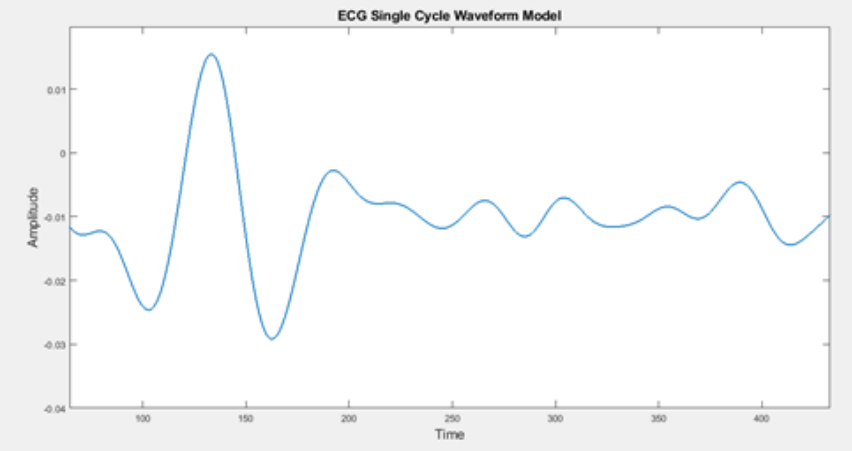

Figure 12. ECG Single cycle model. Source: authors.

2.5. ECG & PPG Feature extraction

Pulse transit time (PTT) is the measurement of the traveling time of blood between two points inside the body and is known to be linearly related to pulse wave velocity (PWV), and is therefore, a function of BP [10,11]. PTT is commonly defined as the time difference between the R-peak in the ECG signal and the next peak of the corresponding PPG cycle [12,13].

Even though PTT as defined above has the potential for continuous and cuffless monitoring of arterial BP because of its linear relation with BP [14,15], most of the current PTT-BP models could provide only one BP parameter.

The following describes an effort to enhance BP estimations. Three different proposals for PTT definition are presented and explained as follows:
a) Peak–to–peak PTT: the peak-to-peak PTT proposed in this research is the time difference between the R-peak of the ECG and the first peek of the PPG. Both signal models are obtained after WT (Figure 13).
b) Peak–to–footpoint PTT: The Peak–to–footpoint PTT is the time delay between the R peak of the ECG model and the foot point of the PPG model (Figure 14).
c) Peak–to–Maximum slope point PTT: is determined as the time interval between the R peak of ECG and the peak of the first derivative of PPG in the same cardiac cycle (Figure 15).

At this step, the first derivative of the PPG model is obtained, and the identification of local maxima gives the position of the peak. The time location of this point is transferred to the PPG signal to obtain the amplitude in the model therefore use it to determine the point for PTT.

BP estimation methods based on PTT have several challenges to be accepted as a feasible method for cuffless monitoring. In terms of implementation, they require the synchronization of two different sensor data (ECG and PPG) coming at different sampling rates in real-time. Additionally, it has been studied [16] that PTT is strongly related to SBP but does not exhibit the same performance while talking about DBP. This is perhaps one reason to decrease the accuracy of predicted BP depending only on the PTT.

On the other hand, information within the PPG waveform is hardly taken into consideration for the measurement of BP. In [17] research discovered that the second peak presented in photoplethysmography (Figure 16) signal would influence the position and the amplitude of the main peak of the original PPG signal and consequently influence the PTT. Consequently, by introducing the information of the PPG second peak in the estimation of BP, the correlation coefficient between the measured and the predicted BP might increase [18, 19].

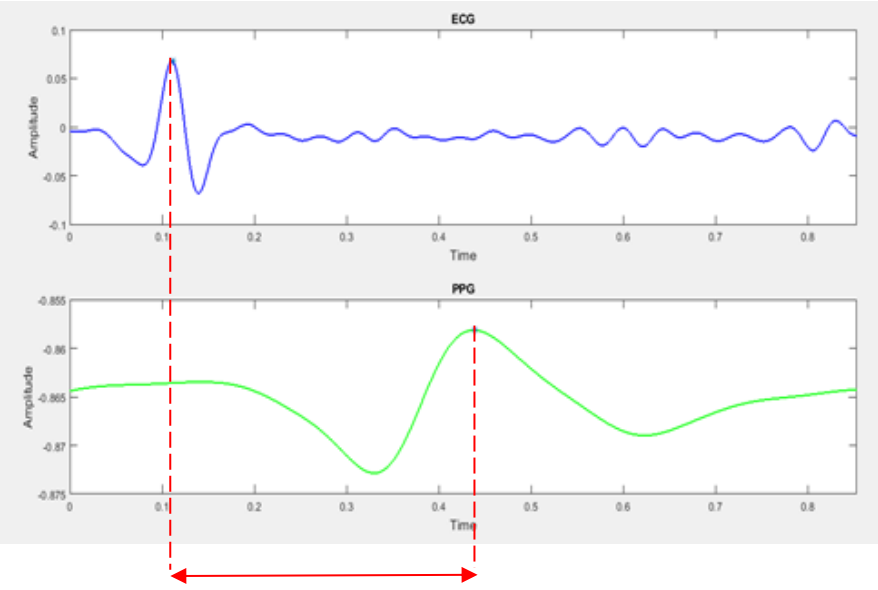

Figure 13. Peak – to – peak PTT. Source: authors.

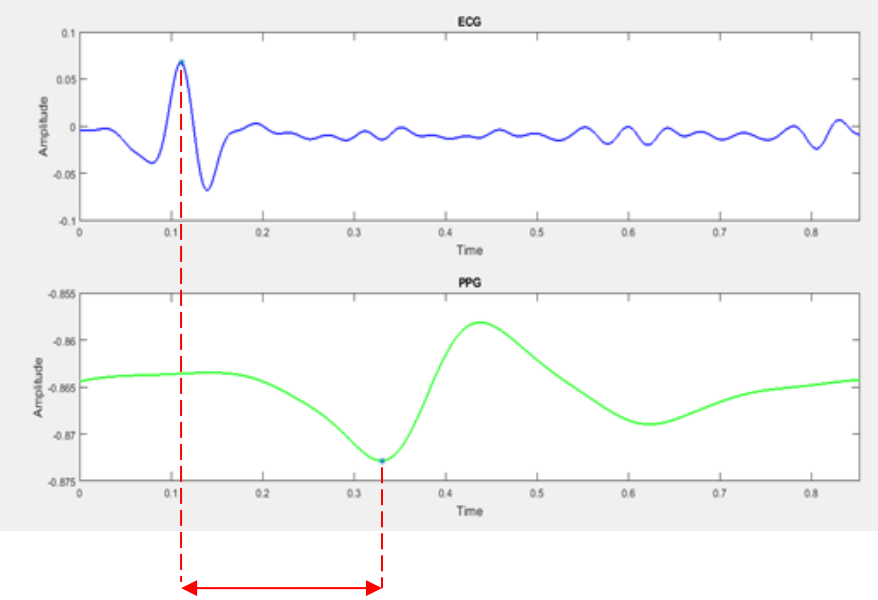

Figure 14. Peak – to – foot point PTT. Source: authors.

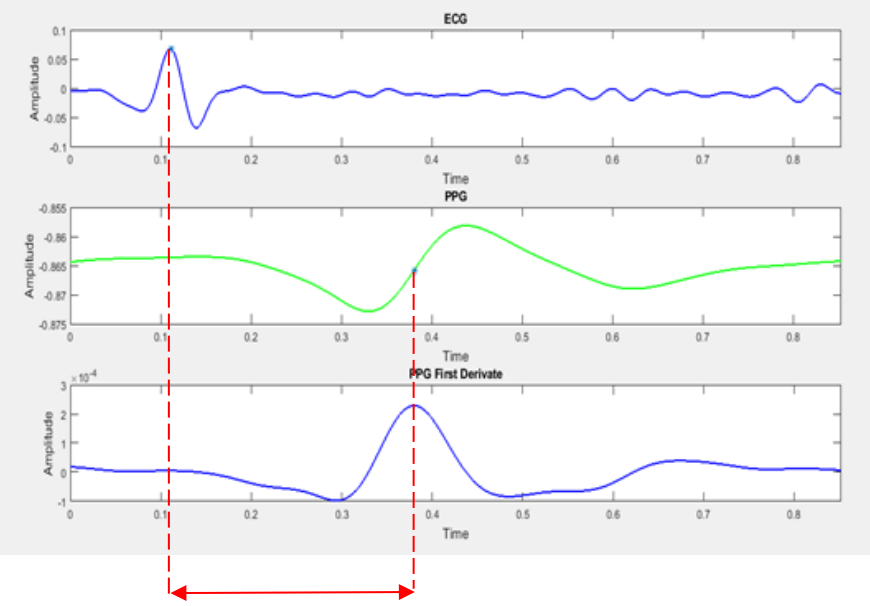

Figure 15. Peak – to – Maximum slope point PTT. Source: authors.

In consideration, the proper identification of the dicrotic notch and the PPG second peak is included in the development of the algorithm for ECG & PPG analysis. PPG first derivative is used to locate inflection points within the PPG signal. The dicrotic notch is identified as the point where the PPG first derivative crosses the zero value from the negative to the positive region (Figure 15).

Additionally, the diastolic peak is established as the subsequent point in which the PPG first derivative crosses the zero value from the negative to the positive region.

Finally, once the dicrotic and secondary peak points are spatially and time located, we proceed to establish the PPG's morphology features for the BP estimation.

a) Ra: this is the amplitude ratio between the first and second peaks about the footpoint in one cycle of the PPG signal (Figure 17).
b) Tsd: represents the period from the first peak to the dicrotic notch.
c) Tfd: identifies the period between the PPG foot point and the dicrotic notch (Figure 18).
d) T1: represents the period from the PPG foot point to the PPG maximum slope point in the same cardiac cycle. It is graphically obtained by constructing a line that best represents the PPG wave before the systolic point and crosses the maximum slope point, the intersection point between this line and the PPG foot point amplitude line is obtained. Therefore, T1 is defined as the time interval between this intersection point and the foot point time (Figure 19).

Summarizing, six-time span indices and one amplitude index are gathered in a data set to build the group of ECG and PPG BP-related parameters. For each patient, a dataset is created. Within each of them, columns represent the seven features separately and row the recorded trials.

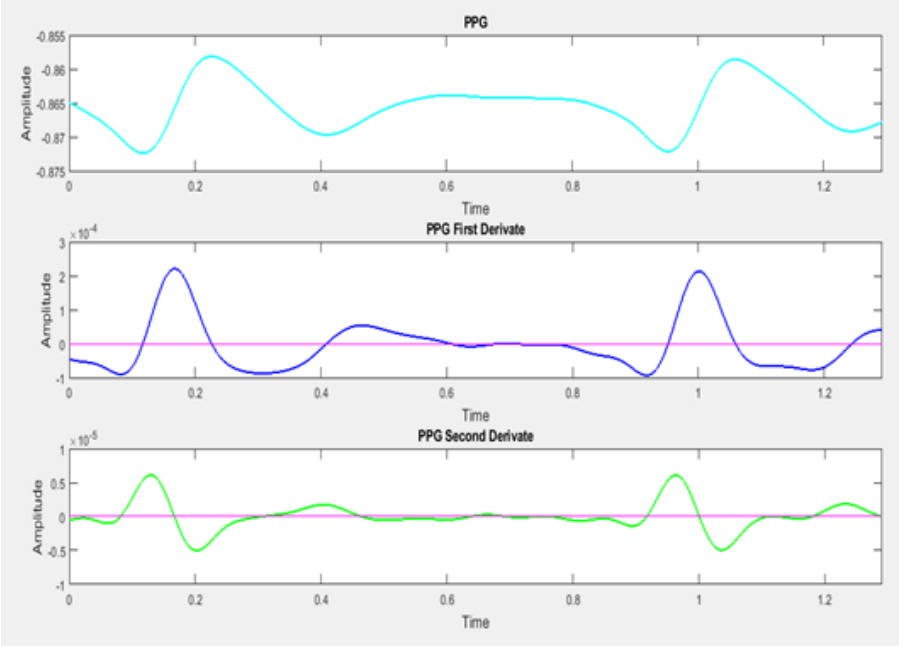

Figure 16. Second peak identification, a – PPG waveform model. b – PPG First derivative. C – PPG Second derivative. Source: authors.

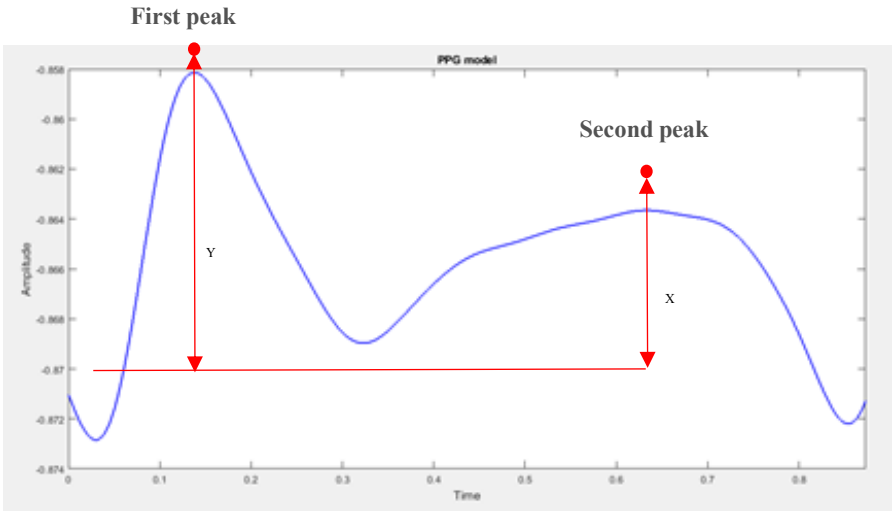

Figure 17. Ra representation. Source: authors.

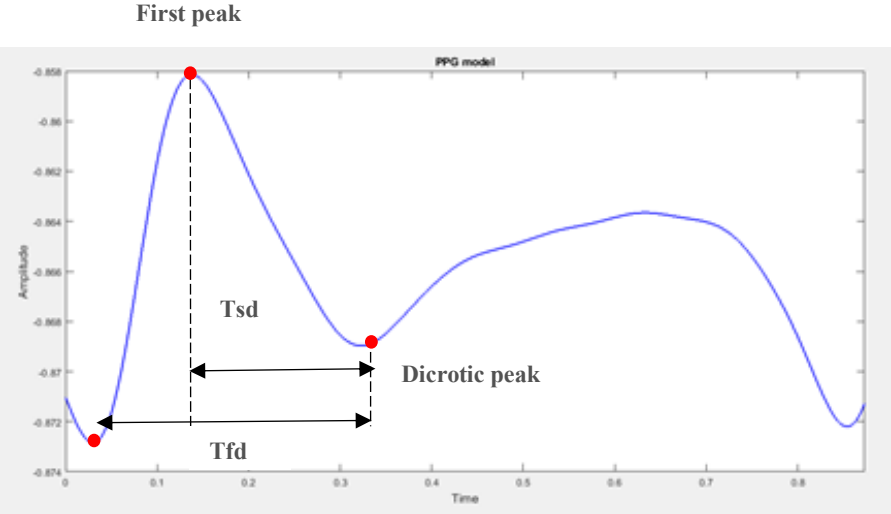

Figure 18. Tsd and Tfd representation. Source: authors.

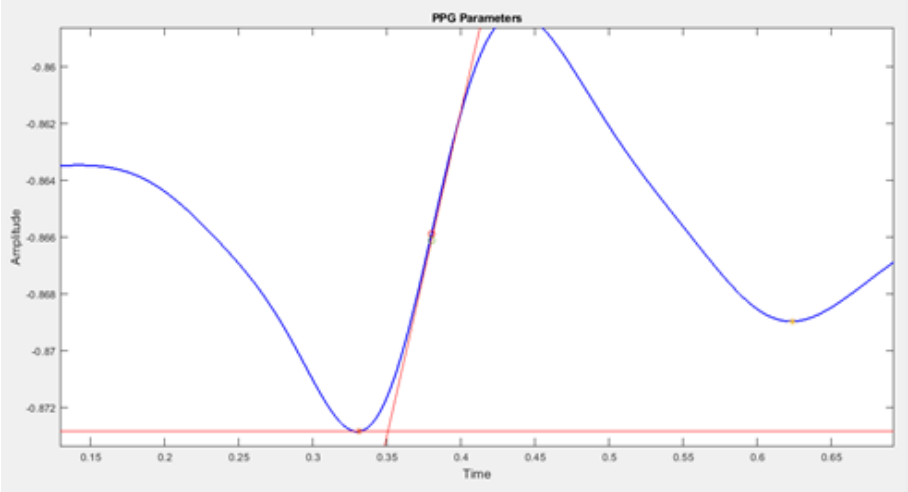

Figure 19. T1 representation. Source: authors.

2.6. Regression analysis

To evaluate the feasibility, the seven PPG and ECG parameters extracted from the processed signal are correlated with the reference SBP and DBP, both components of BP were measured using a standard sphygmomanometer located in patients' upper arm.

For this, an artificial feed-forward neural network with one hidden layer and two output neurons is designed and implemented and the resultant regression line and correlation coefficient between reference and estimated BP are obtained for each patient [20].

3. Results

In Table 1, the patient's health condition is shown in terms of body mass index, measured blood pressure, and estimated heart rate are collected.

The algorithm is tested against eleven patients and the correlation coefficient between the ECG & PPG BP–related parameters and the SBP and DBP is gathered in Table 2.

Table 1. Patient's heart rate, blood pressure and BMI

Patient ID	Heart rate [bpm]	Systolic Blood Pressure SBP [mmHg]	Diastolic Blood Pressure DBP [mmHg]	BMI [Kg/m^2]
P01	54 ± (4.10)	146 ± (16)	76 ± (5.18)	22.9
P02	56± (5.39)	123 ± (13)	75 ± (5.6)	21.7
P03	58 ± (7.29)	131 ± (11.209)	84 ± (7.075)	28.4
P04	64 ± (8.49)	126 ± (11.647)	79 ± (8.709)	34.3
P05	78± (9.14)	112 ± (11.087)	72 ± (11.538)	27.8
P06	67 ± (4.47)	121 ± (14.423)	68 ± (4.745)	30.7
P07	71 ± (7.36)	135 ± (10.524)	85 ± (10.277)	32.1
P08	78 ± (9.66)	119 ± (11.856)	86 ± (7.269)	26.4
P09	88 ± (6.83)	123 ± (12.043)	86 ± (7.869)	25.6
P10	86 ± (8.35)	141 ± (9.961)	92 ± (5.371)	30.8
P11	98 ± (13.6)	134 ± (13.485)	90 ± (8.765)	27.7

Source: authors.

Table 2. Correlation coefficient between reference and estimated blood pressure

Correlation Coefficient R		
Patient ID	Training	General
P01	0,99758	0,95383
P02	0,99563	0,96674
P03	0,99168	0,9583
P04	0,99655	0,97548
P05	0,99322	0,95556
P06	0,98298	0,95701
P07	0,99099	0,95449
P08	0,98426	0,96341
P09	0,99782	0,80218
P10	0,99772	0,94722
P11	0,997	0,97556

Source: authors.

Figure 20 shows the linear regression for reference and estimated blood pressure for one patient.

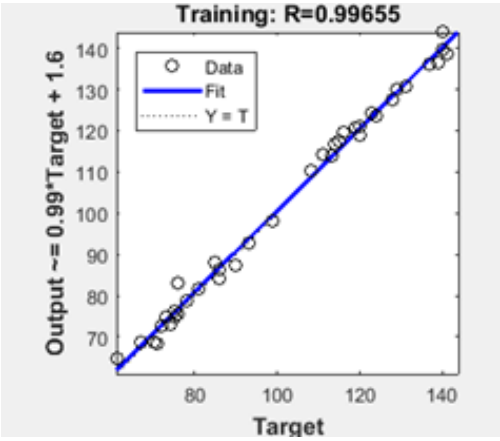

Figure 20. Linear regression reference and estimated BP
Source: authors.

4. Conclusions

The method presented in this work has explored the capability of wavelet analysis as an innovative method for biomedical signal processing. Furthermore, to accomplish the idea of using only PTT for blood pressure estimation, some novel parameters from the PPG's morphology were included in the assessment. The results show a strong correlation between the estimated and reference blood pressure. This opens opportunities for the cuffless estimation of blood pressure.

Although the presented pilot study offers a potential method for cuffless BP measurement, it should be further validated with a larger sample set with the corresponding standard requirement, for example, the IEEE 1708-2004 standard for wearable cuffless BP measuring devices. Moreover, there are still some challenges regarding implementation.

The achieved results provide evidence of advanced estimation of SBP while compared with its respective DBP. It indicates that new parameters directly linked to DBP should be considered to improve the estimation accuracy.

Eventually, BP monitoring in an unobtrusive mobile–based way in which decent accuracy is achieved allows for improved hypertension control, therefore reducing the global burden generated by cardiovascular diseases.

References

[1] "A global brief on hypertension: Silent killer, global public health crisis: World Health Day 2013," *World Health Organization,* 2013. [Online]. Available: https://apps.who.int/iris/handle/10665/79059

[2] M. Elgendi, "On the Analysis of Fingertip Photoplethysmogram Signals," *Current Cardiology Reviews*, vol. 8, no. 1, pp. 14-25, 2012, doi: 10.2174/157340312801215782.

[3] M. Singla, S. Azeemuddin, P. Sistla, "Learning-Based Model for Central Blood Pressure Estimation using Feature Extracted from ECG and PPG signals," in *42a In 2020 42nd Annual International Conference of the IEEE Engineering in Medicine & Biology Society (EMBC),* 2020, pp. 855-858, doi: 10.1109/EMBC44109.2020.9176593.

[4] "CardioQVARK, Control of the cardiovascular system," 2020. [Online]. Available: https://cardioqvark.ru

[5] S. Rezk, C. Join, S. El Asmi, "An algebraic derivative-based method for R wave detection," in *19th European Signal Processing Conference*, 2011, pp. 1578-1582.

[6] J. Hart, "Normal resting pulse rate ranges," *Journal of Nursing Education and Practice*. vol. 5, no. 8, pp. 95-98, 2015, doi: 10.5430/jnep.v5n8p95.

[7] M. Unser, A. Aldroubi, "A review of wavelets in biomedical applications," *Proceedings of the IEEE*, vol. 84, no. 4, pp. 626-638, 1996, doi: https://doi.org/10.1109/5.488704.

[8] M. Singla, P. Sistla, S. Azeemuddin, "Cuff-less Blood Pressure Measurement Using Supplementary ECG and PPG Features Extracted Through Wavelet Transformation," in *41st Annual International Conference of the IEEE Engineering in Medicine and Biology Society (EMBC)*, 2019, pp. 4628-4631, doi: 10.1109/EMBC.2019.8857709.

[9] X. He, RA Goubran, XP Liu, "Secondary Peak Detection of PPG Signal for Continuous Cuffless Arterial Blood Pressure Measurement," *IEEE Transactions on Instrumentation and Measurement*, vol. 63, no. 6, pp. 1431-1439, 2014, doi: 10.1109/TIM.2014.2299524.

[10] S. Datta, R. Banerjee, AD Choudhury, A. Sinha, A. Pal, "Blood pressure estimation from photoplethysmogram using latent parameters," in *IEEE International Conference on Communications (ICC)*, 2016, pp. 1-7, doi: 10.1109/ICC.2016.7511599.

[11] P. Shi, S. Hu, Y. Zhu, J. Zheng, Y. Qiu, P. Cheang, "Insight into the dicrotic notch in photoplethysmographic pulses from the fingertip of young adults," *Journal of medical engineering & technology*, vol. 33, no. 8, pp. 628-633, 2009, doi: 10.3109/03091900903150980.

[12] A. N. Kalinichenko, "Algorithmic support of ECG analysis of the system of remote cardiological monitoring," in *Proceeding of the 20th conference of fruct association*, 2018, pp. 112-117.

[13] M. Chaykovskaya, A. Kalinichenko, E. Fetisova, S. Mironovich, A. Kiprensky, "Artificial Rhythm Recognition Using Portable Cardiomonitor and Mobile Application," in *Proceeding of the 43th Confidence Computing in Cardiology, Vancouver*, 2016, pp. 97-100.

[14] A. N. Kalinichenko, M. K. Chaykovskaya, D. A. Danilova, "Paced ECG Analysis in Mobile Cardiac Monitor," in *Proceedings of the 43rd Conference Computing in Cardiology*, *Vancouver*, 2016, pp. 649-652.

[15] O. B. Сенько and Oleg Sen'ko, "Non-Invasive Arterial Pressure Estimating With the Cardiac Monitor CardioQvark," *Matematicheskaya Biologiya i Bioinformatika*, vol. 12, no 2, pp. 536-545, 2017, doi: 10.17537/2017.12.536.

[16] M. Y. Man Wong, C. C. Yan Poon, and Y. Y. Ting Zhang, "An Evaluation of the Cuffless Blood Pressure Estimation Based on Pulse Transit Time Technique: a Half Year Study on Normotensive Subjects," *Cardiovascular Engineering,* vol. 9, no. 1, pp. 32-38, 2009, doi: 10.1007/s10558-009-9070-7.

[17] X. He, R. A. Goubran, X. P. Liu, "Secondary Peak Detection of PPG Signal for Continuous Cuffless Arterial Blood Pressure Measurement," *IEEE Transactions on Instrumentation and Measurement*, vol. 63, no. 6, pp. 1431-1439, 2014, doi: 10.1109/TIM.2014.2299524.

[18] X. R. Ding, Y. T. Zhang, J. Liu, W. X. Dai, H. K. Tsang, "Continuous Cuffless Blood Pressure Estimation Using Pulse Transit Time and Photoplethysmogram Intensity Ratio," *IEEE Trans. Biomed. Eng.*, vol. 63, no. 5, pp. 964-972, 2016, doi: 10.1109/TBME.2015.2480679

[19] A. I. Khuri, "Introduction to Linear Regression Analysis," *International Statistical Review,* vol. 81, no. 2, pp. 318-319, 2013, doi: 10.1111/insr.12020_10.

[20] M. T. Hagan, H. B. Demuth, M. H. Beale, *Neural Network Design*. Boston, MA, USA: PWS Publishing, 1996.